Applied Physics Express **5** (2012) 062103
DOI: 10.1143/APEX.5.062103

High-Power, Low-Efficiency-Droop Semipolar ($20\bar{2}\bar{1}$) Single-Quantum-Well Blue Light-Emitting Diodes

Chih-Chien Pan[1]*, Shinichi Tanaka[1], Feng Wu[1], Yuji Zhao[2], James S. Speck[1], Shuji Nakamura[1], Steven P. DenBaars[1,2], and Daniel Feezell[1]

[1]*Materials Department, University of California, Santa Barbara, CA 93106-5050, U.S.A.*
[2]*Electrical and Computer Engineering Department, University of California, Santa Barbara, CA 93106-9560, U.S.A.*

Received May 4, 2012; accepted May 20, 2012; published online June 4, 2012

We demonstrate a small-area (0.1 mm^2) semipolar ($20\bar{2}\bar{1}$) blue (447 nm) light-emitting diode (LED) with high light output power (LOP) and external quantum efficiency (EQE) by utilizing a single 12-nm-thick InGaN quantum well. The LED had pulsed LOPs of 140, 253, 361, and 460 mW, and EQEs of 50.1, 45.3, 43.0, and 41.2%, at current densities of 100, 200, 300, and 400 A/cm^2, respectively. The device showed little blue shift and had a narrow full width at half maximum (FWHM). Micro-electroluminescence (μ-EL) and scanning transmission electron microscope (STEM) images indicate a high-quality InGaN quantum well (QW) layer.

Wide-band-gap InGaN/GaN-based light-emitting diodes (LEDs) have attracted considerable attention due to their use in a range of applications for illumination and are often operated at high drive currents to achieve high emission powers. However, current commercial LEDs grown on the *c*-plane of the wurtzite crystal suffer from the quantum-confined Stark effect (QCSE) due to the large polarization-related electric fields.[1)] This effect causes band bending in the active region and results in the spatial separation of the electron and hole wave functions, thus lowering the radiative recombination rate and possibly also reducing the internal quantum efficiency (IQE).[2)] Typically, the quantum wells (QWs) in *c*-plane LEDs are ~3-nm-thick — use of thicker wells usually results in reduced efficiency due to the large separation of electrons and holes in the QWs. Moreover, the IQE is further reduced with increasing injection current by a well-studied but controversial phenomenon known as "efficiency droop".[3–8)] Crystal orientations that have reduced polarization discontinuities between InGaN and GaN, such as the semipolar orientations, or no polarization discontinuity, such as the nonpolar *m*-plane, enable the growth of thick QWs, which results in reduced carrier density in the wells.

Due to the light output power (LOP) rollover observed in polar *c*-plane LEDs at high current densities, large-area (~1 mm^2) chips are typically required in high-power applications to reduce the average operating current density and mitigate the effects of efficiency droop. Alternatively, achieving high-efficiency and low-droop operation at high current densities (>100 A/cm^2) would allow for the implementation of small-area (~0.1 mm^2) chips in high-power applications. This approach would reduce the device footprint and ultimately lead to cost reductions. LEDs grown on nonpolar and semipolar orientations have negligible or reduced polarization-related electric fields, are expected to have higher radiative recombination rates than *c*-plane LEDs, and permit the growth of thicker wells while sustaining high efficiency over a wide range of current densities.[9–11)] In some cases, these devices may show reduced efficiency droop and are therefore potential candidates for the development of small-area, high-power chips. To date, relatively high efficiency violet,[12)] blue-violet,[13)] blue,[14)] and green[15)] LEDs have been demonstrated on free-standing nonpolar or semipolar GaN. In this work, we demonstrate a threefold approach to reduce droop. We utilize the semipolar ($20\bar{2}\bar{1}$) orientation to reduce polarization-related electric fields, a single quantum well (SQW) structure to mitigate carrier nonuniformity issues, and a thick (12 nm) high-quality active region to reduce the average carrier density. With this approach, we realize a small-area, high-power, and low-efficiency-droop blue LED with an external quantum efficiency (EQE) of 50.1% and a LOP of 140 mW at 100 A/cm^2.

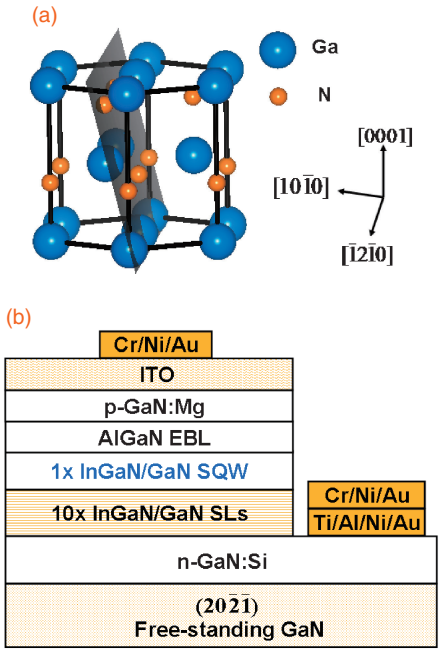

Fig. 1. (a) Schematic figure of the semipolar ($20\bar{2}\bar{1}$) orientation in the wurtzite crystal structure. (b) LED structure on semipolar ($20\bar{2}\bar{1}$) free-standing GaN.

The semipolar ($20\bar{2}\bar{1}$) plane is inclined from the *c*-plane by an angle of 105° and is shown in Fig. 1(a). Figure 1(b) shows the LED structure, which was homoexpitaxially grown on a $5 \times 15\ mm^2$ free-standing semipolar ($20\bar{2}\bar{1}$) substrate using metal organic chemical vapor deposition (MOCVD). The threading dislocation density (TDD) is in the range of 10^5–$10^6\ cm^{-2}$.[16,17)] The structure consisted of a 1-μm-thick Si-doped GaN layer with a Si doping concentration of $1 \times 10^{19}\ cm^{-3}$, followed by a 10-pair $In_{0.01}Ga_{0.99}N$/

*E-mail address: c_pan@umail.ucsb.edu

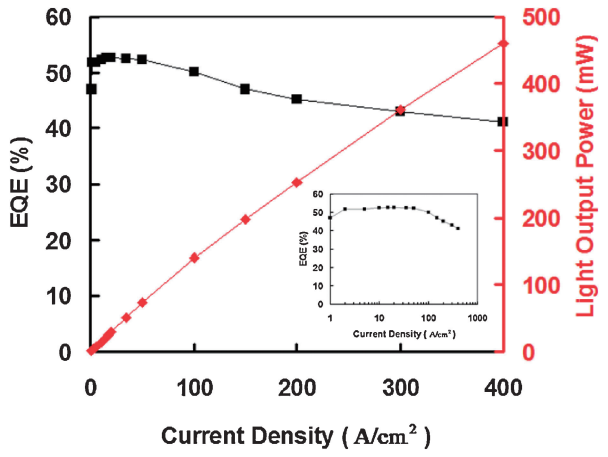

Fig. 2. Light output power and external quantum efficiency vs current density for the semipolar (20$\bar{2}\bar{1}$) blue LED. Inset: Semilog plot of EQE versus current density.

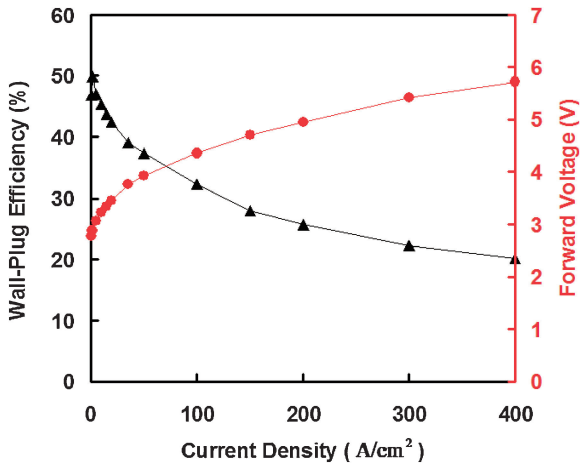

Fig. 3. Wall-plug efficiency and forward voltage for the semipolar (20$\bar{2}\bar{1}$) blue LED.

Table I. EQEs and LOPs of the semipolar (20$\bar{2}\bar{1}$) blue LED at various current densities.

	Current density J (A/cm^2)			
	100	200	300	400
EQE (%)	50.1	45.3	43.0	41.2
LOP (mW)	140	253	361	460

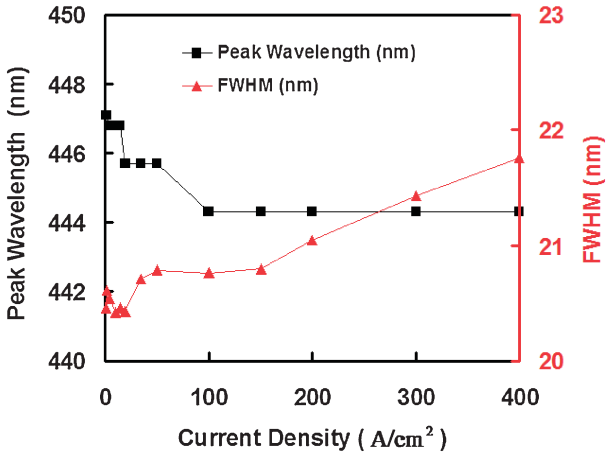

Fig. 4. FWHM and peak wavelength vs current density for the semipolar (20$\bar{2}\bar{1}$) blue LED.

GaN (3/3 nm) superlattice (SL), and a GaN/InGaN/GaN SQW active region consisting of a 10-nm-GaN bottom barrier, a 12-nm-$In_{0.16}Ga_{0.82}N$ quantum well, and a 15-nm-GaN upper barrier. The SQW/barrier layer was followed by a 3-nm-thick $Al_{0.18}Ga_{0.82}N$ electron blocking layer (EBL) with a Mg concentration of 2×10^{19} cm^{-3} and a 50-nm-thick p-type GaN layer with a Mg concentration of 4×10^{19} cm^{-3}. Subsequently, small-area (0.1 mm^2) mesas were formed by chlorine-based reactive ion etching. A 250-nm-thick indium–tin-oxide (ITO) layer was deposited by electron beam evaporation as the transparent p-contact, and Ti/Al/Ni/Au (10/100/10/100 nm) layers were deposited as the n-GaN contact. Finally, a thick Cr/Ni/Au metal stack of 25/20/500 nm was deposited on the ITO and the n-GaN contact to serve as the p-side and n-side wire-bond pads. Encapsulated devices with backside roughening and a ZnO vertical-stand package[14,18] were tested in pulsed mode with a 1 KHz repetition rate and pulse width of 20 μs (2% duty cycle) to prevent self-heating. Device characterization was performed at room temperature with forward currents up to 400 mA.

Figure 2 shows the EQE and LOP of the semipolar (20$\bar{2}\bar{1}$) blue LED vs current density, while Table I lists the EQE and LOP at various current densities. As seen in Table I, the LED had EQEs of 50.1, 45.3, 43.0, and 41.2% at current densities of 100, 200, 300, and 400 A/cm^2, respectively. The corresponding LOPs were 140, 253, 361, and 460 mW at current densities of 100, 200, 300, and 400 A/cm^2, respectively. Figure 3 shows the wall-plug efficiency (WPE) and forward voltage vs current density. The WPE reached a peak value of nearly 50%. The forward voltage was 3.51 V at 20 A/cm^2 and is relatively high compared with that of a commercial device. Transfer length method (TLM) measurements revealed that the p-contact showed rectifying behavior and that the p-GaN resistivity was more than 10 Ω cm. The high forward voltage of the device is attributed to the poor p-contact and the high p-GaN resistivity. Improvements in WPE are expected with the optimization of the p-type layers.

Figure 4 shows the full width at half maximum (FWHM) and peak wavelength vs current density for the semipolar (20$\bar{2}\bar{1}$) blue LED. As seen in Fig. 4, the semipolar (20$\bar{2}\bar{1}$) blue LED had a narrower FWHM than other semipolar or nonpolar planes and a smaller blue shift than LEDs grown on the conventional c-plane or other semipolar and nonpolar planes.[19,20] While the minimal blue shift is partially explained by the cancellation of the piezoelectric field and the pn-junction built-in electric field components, the origin of the narrower FWHM is less clear. The semipolar (20$\bar{2}\bar{1}$) plane shows a high indium incorporation rate compared with other planes, allowing for an increase in the QW growth temperature required to achieve a given emission wavelength. In the blue wavelength regime, the allowed increase in growth temperature is around 35 °C, compared with

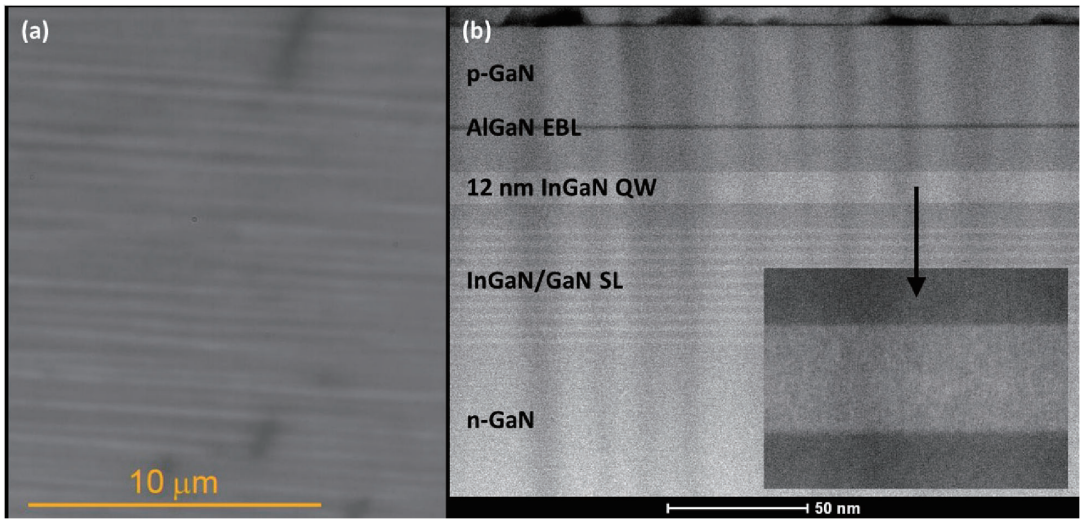

Fig. 5. (a) μ-EL image of the LED. (b) STEM image of the active area of the LED.

semipolar $(20\bar{2}1)$,[21] for example. Typically, increased growth temperatures result in improved InGaN quality, which may explain the narrower FWHM values for the semipolar $(20\bar{2}1)$ QWs (compared with other semipolar planes). Higher growth temperatures may also result in QWs with more compositionally uniform InGaN and fewer QW thickness variations. Figure 5(a) shows a micro-electroluminescence (μ-EL) image of the LED. Very uniform emission from the QW was observed, with few fluctuations in intensity. Some evidence of extended defects is seen in Fig. 5(a) and the origin of these defects is under investigation. Some morphological features were also observed on the surface. Figure 5(b) shows a scanning transmission electron microscope (STEM) image of the active area of the LED taken along the projection of the *c*-axis. The STEM image reveals smooth QW interfaces and uniform QW thickness. Based on the small blue shift and narrow spectral width shown in Fig. 4 (and in previously published results[13,22]) and the μ-EL and STEM images showing uniform QW emission and smooth QW interfaces, we propose that InGaN QWs on the semipolar $(20\bar{2}1)$ plane are relatively free from potential fluctuations. This results in a low degree of carrier localization and minimal band filling of localized states.[23,24] Ryu *et al.*[25] have recently postulated that polarization related-electric fields,[1] nonuniform carrier distribution,[26] and potential fluctuations[27] significantly reduce the effective active region volume over which carriers are distributed in conventional *c*-plane InGaN QWs. As a result, high carrier densities are present in the active region, which exacerbate the effects of Auger recombination and carrier leakage,[3,8,28] resulting in efficiency droop. In our semipolar $(20\bar{2}1)$ LEDs, polarization-related electric fields are significantly reduced, a SQW active region eliminates carrier nonuniformity issues, and a thick high-quality InGaN layer reduces the effects of potential fluctuations and lowers the average carrier density. This reduces the effects of Auger recombination and carrier leakage, resulting in a device with low efficiency droop.

In summary, we achieved a high-power and low-efficiency-droop blue semipolar $(20\bar{2}1)$ LED by utilizing a high-quality 12-nm-thick SQW active region. This device exhibited EQEs of 50.1, 45.3, 43.0, and 41.2% and LOPs of 140, 253, 361, and 460 mW at current densities of 100, 200, 300, and 400 A/cm^2, respectively. Wall-plug efficiencies near 50% were also demonstrated. The semipolar $(20\bar{2}1)$ blue LED showed a very small blue shift and a narrow FWHM. We also presented a μ-EL image that indicates uniform emission from the QW and an STEM image showing smooth QW interfaces and uniform QW thickness for this device. The combination of low polarization-related electric fields, an SQW structure, and a thick high-quality InGaN layer results in low efficiency droop.

Acknowledgments The authors would like to thank Fabian Rol from Cree, Inc. The authors acknowledge the Solid-State Lighting and Energy Center (SSLEC) at UCSB and the support of the NSF MRSEC program (DMR 1121053) for MRL characterization facilities. A portion of this work was performed in the UCSB nanofabrication facility, part of the National Science Foundation (NSF)—funded National Nanotechnology Infrastructure Network (NNIN).

1) F. Bernardini *et al.*: Phys. Rev. B **56** (1997) 10024.
2) V. Fiorentini and F. Bernardini: Phys. Rev. B **60** (1999) 8849.
3) E. Kioupakis *et al.*: Appl. Phys. Lett. **98** (2011) 161107.
4) J. Hader *et al.*: Appl. Phys. Lett. **96** (2010) 221106.
5) A. David and M. J. Grundmann: Appl. Phys. Lett. **96** (2010) 103504.
6) J. Piprek: Phys. Status Solidi A **207** (2010) 2217.
7) X. Ni *et al.*: J. Appl. Phys. **108** (2010) 033112.
8) M. H. Kim *et al.*: Appl. Phys. Lett. **91** (2007) 183507.
9) P. Waltereit *et al.*: Nature **406** (2000) 865.
10) S. H. Park: J. Appl. Phys. **93** (2003) 9665.
11) W. G. Scheibenzuber *et al.*: Phys. Rev. B **80** (2009) 115320.
12) K. C. Kim *et al.*: Appl. Phys. Lett. **91** (2007) 181120.
13) Y. Zhao *et al.*: Appl. Phys. Express **4** (2011) 082104.
14) Y. Zhao *et al.*: Appl. Phys. Express **3** (2010) 102101.
15) S. Yamamoto *et al.*: Appl. Phys. Express **3** (2010) 122102.
16) P. S. Hsu *et al.*: Appl. Phys. Lett. **99** (2011) 081912.
17) K. Fujito *et al.*: Phys. Status Solidi A **205** (2008) 1056.
18) C. C. Pan *et al.*: Jpn. J. Appl. Phys. **49** (2010) 080210.
19) Y. D. Lin *et al.*: Appl. Phys. Lett. **94** (2009) 261108.
20) H. Zhong *et al.*: Electron. Lett. **43** (2007) 15.
21) Y. Zhao *et al.*: Appl. Phys. Lett. **100** (2012) 201108.
22) C. Y. Huang *et al.*: Appl. Phys. Lett. **99** (2011) 241115.
23) S. Chichibu *et al.*: Appl. Phys. Lett. **69** (1996) 4188.
24) Y. Narukawa *et al.*: Appl. Phys. Lett. **70** (1997) 981.
25) H. Y. Ryu *et al.*: Appl. Phys. Lett. **100** (2012) 131109.
26) A. David *et al.*: Appl. Phys. Lett. **92** (2008) 053502.
27) S. F. Chicuibu *et al.*: Nat. Mater. **5** (2006) 810.
28) Y. C. Shen *et al.*: Appl. Phys. Lett. **91** (2007) 141101.